Supplement of Biogeosciences, 12, 3953–3971, 2015
http://www.biogeosciences.net/12/3953/2015/
doi:10.5194/bg-12-3953-2015-supplement

Biogeosciences Open Access

Supplement of

Carbon export and transfer to depth across the Southern Ocean Great Calcite Belt

S. Z. Rosengard et al.

Correspondence to: S. Z. Rosengard (srosengard@whoi.edu); P. J. Lam (pjlam@ucsc.edu)

Supplement Contents

This supplement contains, in the following order:

Table S1. ^{234}Th activity and flux profiles estimated at 27 stations along cruises GB1 and GB2. Fluxes were estimated by measuring total seawater ^{234}Th activity deficits relative to total seawater ^{238}U activity, as described in Sect. 2.4. ^{234}Th flux errors are propagated from ^{234}Th activity errors.

Cruise	Station	Depth	^{234}Th Activity	^{234}Th Activity Error	^{238}U Activity	^{234}Th Flux	^{234}Th Flux Error
-	-	*m*	*dpm L^{-1}*	*dpm L^{-1}*	*dpm L^{-1}*	*dpm m^{-2} d^{-1}*	*dpm m^{-2} d^{-1}*
GB1	6	13.6	1.04	0.02	2.36	681	27
GB1	6	22.3	1.28	0.05	2.36	924	31
GB1	6	29.2	1.12	0.03	2.36	1,243	34
GB1	6	40.2	1.23	0.03	2.36	1,503	37
GB1	6	45.2	1.29	0.06	2.36	1,702	39
GB1	6	53.1	1.53	0.04	2.36	2,096	48
GB1	6	78	1.86	0.12	2.36	2,437	100
GB1	6	100.6	1.90	0.05	2.36	2,684	106
GB1	6	115	2.08	0.10	2.36	2,804	116
GB1	6	130	2.15	0.05	2.36	2,911	121
GB1	6	150.3	2.09	0.07	2.36	3,182	145
GB1	6	200	2.04	0.18	2.37	3,419	195
GB1	16	11.1	0.99	0.02	2.35	548	20
GB1	16	17.07	1.10	0.02	2.35	762	22
GB1	16	23.04	0.94	0.02	2.35	1,107	25
GB1	16	34.2	1.61	0.04	2.35	1,311	30
GB1	16	42.2	1.61	0.05	2.36	1,611	42
GB1	16	62.3	1.97	0.05	2.36	1,933	71
GB1	16	100.17	2.06	0.05	2.36	2,277	105
GB1	16	140.8	2.18	0.06	2.37	2,487	139
GB1	16	180.1	2.24	0.08	2.37	2,636	178
GB1	16	220.5	2.21	0.21	2.37	2,819	308
GB1	16	260.7	2.37	0.13	2.37	2,810	394
GB1	16	340.3	2.16	0.08	2.37	3,040	409
GB1	25	10.3	1.70	0.05	2.45	283	26
GB1	25	16.1	1.95	0.06	2.45	380	30
GB1	25	23.8	1.91	0.03	2.45	525	34
GB1	25	34.5	2.14	0.05	2.47	611	38
GB1	25	41.7	2.07	0.07	2.47	773	51
GB1	25	80	2.42	0.03	2.48	941	74
GB1	25	115	2.46	0.04	2.45	937	91
GB1	25	140.5	2.38	0.05	2.43	975	103
GB1	25	165.2	2.32	0.07	2.44	1,074	125
GB1	25	200.2	2.44	0.04	2.42	1,029	177

GB1	25	300	2.36	0.03	2.38	1,051	195
GB1	32	12.15	1.96	0.08	2.48	229	41
GB1	32	18	1.96	0.06	2.48	327	44
GB1	32	25.25	2.00	0.07	2.49	475	51
GB1	32	39.2	2.02	0.10	2.49	614	61
GB1	32	46	2.05	0.19	2.49	808	104
GB1	32	69.67	1.83	0.04	2.47	1,304	116
GB1	32	100.2	2.33	0.03	2.48	1,435	127
GB1	32	130.5	2.38	0.03	2.47	1,520	141
GB1	32	171	2.41	0.09	2.46	1,581	186
GB1	32	210	2.43	0.03	2.46	1,612	198
GB1	32	251	2.29	0.11	2.45	1,818	250
GB1	32	300.8	2.52	0.03	2.44	1,761	253
GB1	38	20.4	2.36	0.08	2.52	127	72
GB1	38	32.2	2.17	0.03	2.52	247	74
GB1	38	44.2	2.20	0.04	2.52	418	83
GB1	38	69	2.28	0.10	2.53	550	102
GB1	38	81	2.27	0.08	2.54	638	107
GB1	38	92	2.34	0.03	2.53	743	113
GB1	38	121	2.43	0.05	2.51	809	126
GB1	38	150	2.41	0.09	2.50	886	151
GB1	38	175	2.57	0.05	2.50	811	168
GB1	38	220	2.43	0.06	2.50	911	206
GB1	38	280.2	2.47	0.05	2.48	938	247
GB1	38	350.7	2.74	0.08	2.48	678	265
GB1	46	10	1.40	0.02	2.43	395	20
GB1	46	16.8	1.47	0.03	2.43	573	23
GB1	46	23	1.54	0.03	2.43	813	28
GB1	46	35.7	1.41	0.02	2.42	1,090	32
GB1	46	42.03	1.37	0.02	2.42	1,338	34
GB1	46	52.1	1.36	0.03	2.42	1,652	38
GB1	46	62.7	1.74	0.07	2.42	2,123	69
GB1	46	100.4	2.44	0.03	2.41	2,089	102
GB1	46	150.4	2.51	0.05	2.40	1,937	146
GB1	46	200.4	2.46	0.05	2.40	1,850	174
GB1	46	250.2	2.37	0.11	2.39	1,874	283
GB1	46	325.3	2.53	0.12	2.38	1,712	314
GB1	59	10.4	1.46	0.03	2.34	335	21
GB1	59	16.1	1.43	0.06	2.34	493	25
GB1	59	22.5	1.64	0.21	2.34	673	61
GB1	59	34	1.61	0.12	2.34	857	69
GB1	59	40	1.50	0.03	2.34	1,013	70
GB1	59	47	1.49	0.05	2.34	1,256	73

GB1	59	60	1.49	0.09	2.34	1,844	102
GB1	59	95	2.12	0.05	2.35	2,108	128
GB1	59	140	2.05	0.06	2.36	2,509	159
GB1	59	185	2.24	0.09	2.37	2,673	202
GB1	59	225	2.16	0.05	2.37	3,113	244
GB1	59	325	2.34	0.04	2.40	3,189	262
GB1	70	17	1.86	0.06	2.36	314	47
GB1	70	27	1.85	0.06	2.36	460	52
GB1	70	37	1.76	0.05	2.36	721	61
GB1	70	57.5	1.81	0.06	2.36	967	69
GB1	70	68	1.90	0.05	2.37	1,119	72
GB1	70	80	2.05	0.05	2.37	1,266	80
GB1	70	100	2.36	0.06	2.38	1,280	94
GB1	70	125	2.29	0.18	2.38	1,361	190
GB1	70	160	2.35	0.06	2.39	1,412	208
GB1	70	200	2.40	0.09	2.40	1,414	248
GB1	70	250	2.45	0.09	2.40	1,342	286
GB1	70	300	2.27	0.06	2.41	1,439	292
GB1	77	17	1.71	0.06	2.35	399	45
GB1	77	26	1.68	0.05	2.35	573	49
GB1	77	35	1.84	0.05	2.35	794	57
GB1	77	56	1.79	0.06	2.35	1,047	66
GB1	77	66	1.86	0.06	2.35	1,197	70
GB1	77	77	1.97	0.06	2.36	1,391	79
GB1	77	101	2.25	0.08	2.37	1,485	105
GB1	77	130	2.30	0.06	2.39	1,561	122
GB1	77	160	2.31	0.06	2.39	1,630	139
GB1	77	190	2.16	0.05	2.40	1,903	162
GB1	77	240	2.40	0.07	2.40	1,917	213
GB1	77	300	2.40	0.13	2.41	1,922	243
GB1	85	12.6	1.30	0.05	2.35	476	32
GB1	85	19	1.55	0.07	2.35	629	35
GB1	85	26	1.41	0.06	2.35	925	43
GB1	85	41	1.52	0.07	2.35	1,197	52
GB1	85	49	1.76	0.07	2.35	1,340	56
GB1	85	58	1.91	0.07	2.35	1,493	63
GB1	85	73	1.86	0.08	2.35	1,858	94
GB1	85	110	2.17	0.09	2.36	2,034	133
GB1	85	140	2.34	0.09	2.36	2,059	168
GB1	85	180	2.36	0.09	2.37	2,076	207
GB1	85	220	2.46	0.09	2.38	1,931	273
GB1	85	300	2.60	0.10	2.39	1,683	300
GB1	92	10	1.68	0.07	2.34	239	32

GB1	92	15	1.61	0.07	2.34	365	35
GB1	92	22	1.54	0.07	2.34	571	41
GB1	92	33	1.78	0.04	2.34	709	43
GB1	92	39	1.65	0.05	2.34	837	45
GB1	92	46	1.59	0.04	2.34	1,053	48
GB1	92	59	1.59	0.06	2.34	1,639	77
GB1	92	100	2.65	0.07	2.35	1,332	117
GB1	92	130	2.28	0.06	2.36	1,396	134
GB1	92	160	2.41	0.09	2.36	1,339	170
GB1	92	200	2.42	0.06	2.37	1,248	232
GB1	92	302	2.29	0.06	2.38	1,391	259
GB1	101	13.6	1.57	0.04	2.36	405	33
GB1	101	22	1.46	0.04	2.36	611	35
GB1	101	29.5	1.58	0.05	2.36	867	42
GB1	101	45	1.61	0.05	2.36	1,133	49
GB1	101	54	1.74	0.06	2.37	1,296	52
GB1	101	63	1.89	0.06	2.37	1,484	61
GB1	101	81	1.96	0.07	2.37	1,763	82
GB1	101	110	2.24	0.07	2.38	1,878	107
GB1	101	140	2.43	0.05	2.37	1,826	122
GB1	101	171	2.43	0.05	2.37	1,774	135
GB1	101	200	2.44	0.05	2.37	1,641	184
GB1	101	300	2.20	0.04	2.37	1,883	205
GB1	109	11.1	1.58	0.03	2.39	318	23
GB1	109	16.2	1.69	0.04	2.39	445	25
GB1	109	23.7	1.62	0.04	2.39	672	31
GB1	109	36.5	1.77	0.04	2.40	854	35
GB1	109	44	1.76	0.04	2.48	1,158	44
GB1	109	66	2.03	0.04	2.40	1,326	53
GB1	109	76	1.99	0.04	2.40	1,524	61
GB1	109	100	2.17	0.04	2.39	1,648	71
GB1	109	115	2.19	0.04	2.40	1,737	76
GB1	109	130	2.43	0.05	2.40	1,722	83
GB1	109	150	2.40	0.05	2.40	1,719	94
GB1	109	175	2.40	0.05	2.40	1,719	97
GB1	117	10.5	1.80	0.04	2.43	243	24
GB1	117	16.3	1.69	0.03	2.43	377	26
GB1	117	23	1.99	0.04	2.43	484	30
GB1	117	33	1.77	0.04	2.41	659	34
GB1	117	42	1.95	0.04	2.41	758	37
GB1	117	48	1.86	0.04	2.42	918	41
GB1	117	62	1.87	0.04	2.43	1,177	50
GB1	117	80	2.08	0.04	2.44	1,346	58

GB1	117	95	2.31	0.05	2.44	1,404	65
GB1	117	110	2.46	0.05	2.44	1,394	71
GB1	117	125	2.61	0.05	2.43	1,290	82
GB1	117	150	2.52	0.05	2.43	1,258	86
GB2	5	20	1.37	6.03	2.47	948	5,206
GB2	5	40	1.70	0.08	2.47	1,403	5,206
GB2	5	61	1.84	0.07	2.47	1,768	5,206
GB2	5	71	1.89	0.15	2.48	2,015	5,206
GB2	5	80	2.18	0.07	2.47	1,889	5,207
GB2	5	90	2.56	0.07	2.47	1,862	5,207
GB2	5	100	2.52	0.08	2.48	1,850	5,207
GB2	5	111	2.54	0.08	2.47	1,832	5,207
GB2	5	120	2.44	0.09	2.47	1,849	5,207
GB2	5	150	2.50	0.07	2.48	1,821	5,208
GB2	5	201	2.82	0.14	2.47	1,058	5,218
GB2	5	300	2.71	0.09	2.46	695	5,220
GB2	27	20	1.70	0.04	2.34	554	53
GB2	27	40	1.56	0.04	2.34	1,114	69
GB2	27	70	1.68	0.06	2.34	1,637	92
GB2	27	85	1.53	0.24	2.34	2,047	155
GB2	27	95	1.97	0.05	2.34	1,828	159
GB2	27	105	2.20	0.06	2.35	1,869	160
GB2	27	115	2.21	0.08	2.35	1,910	162
GB2	27	125	2.28	0.06	2.35	1,931	164
GB2	27	135	2.27	0.05	2.35	1,972	168
GB2	27	160	2.18	0.06	2.35	2,130	181
GB2	27	200	2.41	0.06	2.36	2,063	205
GB2	27	250	2.69	0.08	2.36	1,826	216
GB2	36	20	1.83	0.04	2.34	434	55
GB2	36	40	1.86	0.06	2.34	639	65
GB2	36	50	1.82	0.08	2.34	824	73
GB2	36	65	1.91	0.05	2.34	981	77
GB2	36	75	2.19	0.08	2.35	1,035	84
GB2	36	90	2.48	0.06	2.35	988	89
GB2	36	100	2.29	0.08	2.35	1,034	117
GB2	36	125	2.04	0.07	2.35	1,372	148
GB2	36	150	2.23	0.06	2.35	1,161	169
GB2	36	175	2.42	0.06	2.35	1,110	178
GB2	36	200	2.39	0.05	2.36	1,077	194
GB2	36	250	2.58	0.07	2.36	923	202
GB2	43	20	1.89	0.04	2.33	383	55
GB2	43	40	1.90	0.08	2.33	632	76
GB2	43	60	1.93	0.08	2.33	896	99

GB2	43	85	2.06	0.07	2.34	1,034	108
GB2	43	95	2.03	0.05	2.34	1,147	111
GB2	43	110	2.17	0.24	2.34	1,221	153
GB2	43	125	2.25	0.05	2.34	1,258	156
GB2	43	140	2.25	0.10	2.34	1,308	169
GB2	43	165	2.45	0.06	2.34	1,233	177
GB2	43	190	2.35	0.06	2.35	1,230	186
GB2	43	220	2.33	0.07	2.35	1,247	200
GB2	43	250	2.68	0.09	2.36	1,108	205
GB2	53	20	1.87	0.08	2.34	407	80
GB2	53	40	1.88	0.14	2.34	668	117
GB2	53	60	1.99	0.05	2.34	915	126
GB2	53	90	1.98	0.05	2.34	1,120	132
GB2	53	100	2.27	0.08	2.34	1,139	134
GB2	53	110	2.45	0.06	2.34	1,109	136
GB2	53	120	2.40	0.06	2.34	1,056	151
GB2	53	170	2.38	0.11	2.35	1,013	220
GB2	53	210	2.52	0.06	2.35	827	237
GB2	53	250	2.30	0.06	2.36	860	241
GB2	63	20	1.88	0.09	2.34	394	88
GB2	63	40	1.94	0.08	2.34	625	102
GB2	63	60	1.95	0.08	2.34	848	115
GB2	63	80	1.92	0.05	2.34	1,089	121
GB2	63	100	2.12	0.13	2.34	1,187	135
GB2	63	110	2.20	0.08	2.34	1,229	138
GB2	63	120	2.25	0.10	2.34	1,285	151
GB2	63	130	2.31	0.10	2.34	1,316	174
GB2	63	150	2.37	0.09	2.35	1,267	191
GB2	63	175	2.38	0.09	2.35	1,248	204
GB2	63	200	2.32	0.14	2.36	1,292	262
GB2	63	250	2.50	0.09	2.37	1,198	272
GB2	73	20	1.80	0.06	2.35	433	63
GB2	73	35	1.79	0.06	2.35	675	71
GB2	73	50	1.94	0.09	2.35	823	79
GB2	73	60	1.96	0.07	2.35	966	85
GB2	73	75	2.30	0.11	2.37	997	99
GB2	73	90	2.43	0.09	2.38	977	108
GB2	73	105	2.63	0.07	2.39	822	120
GB2	73	120	2.58	0.12	2.39	677	156
GB2	73	135	2.43	0.06	2.40	794	168
GB2	73	160	2.34	0.06	2.40	853	184
GB2	73	200	2.48	0.06	2.40	807	189
GB2	87	20	1.93	0.07	2.35	354	71

GB2	87	40	1.92	0.05	2.35	599	81
GB2	87	60	1.75	0.06	2.35	939	91
GB2	87	80	1.89	0.07	2.35	1,134	98
GB2	87	90	1.88	0.05	2.35	1,268	100
GB2	87	100	2.28	0.08	2.35	1,290	103
GB2	87	110	2.33	0.13	2.35	1,299	115
GB2	87	125	2.35	0.08	2.36	1,302	121
GB2	87	140	2.36	0.08	2.36	1,297	136
GB2	87	170	2.32	0.08	2.36	1,336	159
GB2	87	200	2.48	0.09	2.37	1,213	196
GB2	87	250	2.55	0.08	2.38	1,088	208
GB2	93	20	1.95	0.07	2.36	352	71
GB2	93	40	2.04	0.09	2.36	554	96
GB2	93	65	2.14	0.08	2.36	710	116
GB2	93	90	1.95	0.08	2.36	944	127
GB2	93	105	2.01	0.08	2.36	1,071	132
GB2	93	115	2.17	0.10	2.37	1,142	137
GB2	93	130	2.57	0.09	2.39	1,061	144
GB2	93	145	2.44	0.08	2.39	1,033	152
GB2	93	165	2.42	0.08	2.39	1,003	170
GB2	93	180	2.40	0.09	2.39	992	213
GB2	93	200	2.82	0.09	2.39	469	249
GB2	93	250	2.61	0.09	2.38	309	259
GB2	100	20	1.89	0.05	2.42	464	58
GB2	100	40	1.90	0.07	2.42	764	75
GB2	100	60	2.06	0.07	2.42	922	83
GB2	100	70	1.80	0.05	2.42	1,101	85
GB2	100	80	2.27	0.08	2.43	1,145	89
GB2	100	90	2.33	0.08	2.43	1,174	94
GB2	100	100	2.66	0.28	2.43	1,110	124
GB2	100	110	2.43	0.08	2.43	1,112	130
GB2	100	130	2.30	0.09	2.43	1,205	151
GB2	100	160	2.48	0.09	2.43	1,157	182
GB2	100	200	2.47	0.08	2.43	1,132	190
GB2	106	20	1.87	0.05	2.47	603	68
GB2	106	50	1.77	0.05	2.47	1,005	79
GB2	106	60	1.83	0.06	2.47	1,189	82
GB2	106	70	2.09	0.08	2.48	1,301	86
GB2	106	80	2.17	0.08	2.48	1,413	92
GB2	106	95	2.45	0.09	2.48	1,426	107
GB2	106	115	2.62	0.09	2.48	1,335	126
GB2	106	140	2.50	0.06	2.48	1,320	138
GB2	106	165	2.36	0.06	2.48	1,423	154

GB2	106	200	2.49	0.07	2.47	1,405	186
GB2	106	250	2.64	0.17	2.46	1,274	226
GB2	112	10	2.11	0.08	2.42	136	40
GB2	112	20	2.39	0.09	2.42	149	54
GB2	112	35	2.29	0.08	2.42	199	65
GB2	112	45	1.91	0.07	2.43	347	69
GB2	112	55	1.80	0.07	2.42	526	73
GB2	112	65	2.25	0.09	2.42	589	82
GB2	112	80	2.20	0.08	2.43	717	97
GB2	112	105	2.47	0.09	2.43	682	126
GB2	112	135	2.66	0.09	2.42	466	160
GB2	112	170	2.63	0.09	2.42	270	186
GB2	112	200	2.69	0.10	2.42	-39	223
GB2	112	250	2.66	0.10	2.42	-211	237
GB2	119	10	1.73	0.19	2.42	347	96
GB2	119	25	1.73	0.05	2.42	644	101
GB2	119	40	1.77	0.06	2.42	923	106
GB2	119	55	2.00	0.07	2.42	1,072	110
GB2	119	65	2.16	0.07	2.43	1,147	113
GB2	119	74	2.21	0.07	2.43	1,226	117
GB2	119	90	2.43	0.08	2.43	1,223	124
GB2	119	105	2.32	0.08	2.42	1,280	135
GB2	119	130	2.60	0.08	2.43	1,127	158
GB2	119	165	2.69	0.09	2.42	853	189
GB2	119	200	2.50	0.08	2.42	756	218
GB2	119	250	2.75	0.09	2.42	516	231

Table S2. ^{234}Th and POC fluxes at $z_{Th/U}$, estimated at 27 stations along cruises GB1 and GB2. $z_{Th/U}$ is the depth where ^{234}Th and ^{238}U activities re-establish secular equilibrium. Calculations of POC flux from ^{234}Th fluxes are described in Sect. 2.4. POC flux errors are propagated from ^{234}Th flux, and POC:^{234}Th errors.

Cruise	Station	$z_{Th/U}$	^{234}Th Flux	^{234}Th Flux Error	>51µm POC:^{234}Th	POC Flux	POC Flux Error
-	-	*m*	*dpm m^{-2} d^{-1}*	*dpm m^{-2} d^{-1}*	*µmol dpm^{-1}*	*mmol m^{-2} d^{-1}*	*mmol m^{-2} d^{-1}*1
GB1	6	130	2,911	121	2.0	5.7	0.25
GB1	16	140.8	2,487	139	2.6	6.6	0.37
GB1	25	115	937	91	1.7	1.6	0.18
GB1	32	131	1,581	186	1.3	2.0	0.20
GB1	38	121	809	126	2.7	2.2	0.35
GB1	46	100	2,089	102	2.8	5.9	0.32
GB1	59	95	2,108	128	2.9	6.1	0.42
GB1	70	100	1,280	94	4.3	5.5	0.44
GB1	77	100	1,485	105	6.0	9.0	1.3
GB1	85	140	2,059	168	5.9	12	1.0
GB1	92	100	1,332	117	3.8	5.1	0.47
GB1	101	140	1,826	122	1.8	3.3	0.23
GB1	109	130	1,722	83	1.0	1.6	0.09
GB1	117	110	1,394	71	1.0	1.4	0.09
GB2	5	90	1,862	5,207	1.3	2.5	6.9
GB2	27	105	1,869	160	1.9	3.5	0.32
GB2	36	90	988	89	2.0	2.0	0.18
GB2	43	125	1,258	156	3.7	4.6	0.58
GB2	53	100	1,139	134	3.9	4.4	0.53
GB2	63	130	1,316	174	4.6	6.1	0.81
GB2	73	75	997	99	4.9	4.9	0.49
GB2	87	100	1,290	103	2.9	3.8	0.33
GB2	93	130	1,061	144	1.2	1.2	0.18
GB2	100	90	1,174	94	2.8	3.3	0.27
GB2	106	95	1,426	107	0.9	1.2	0.10
GB2	112	105	682	126	0.8	0.6	0.11
GB2	119	90	1,223	124	2.5	3.0	0.31

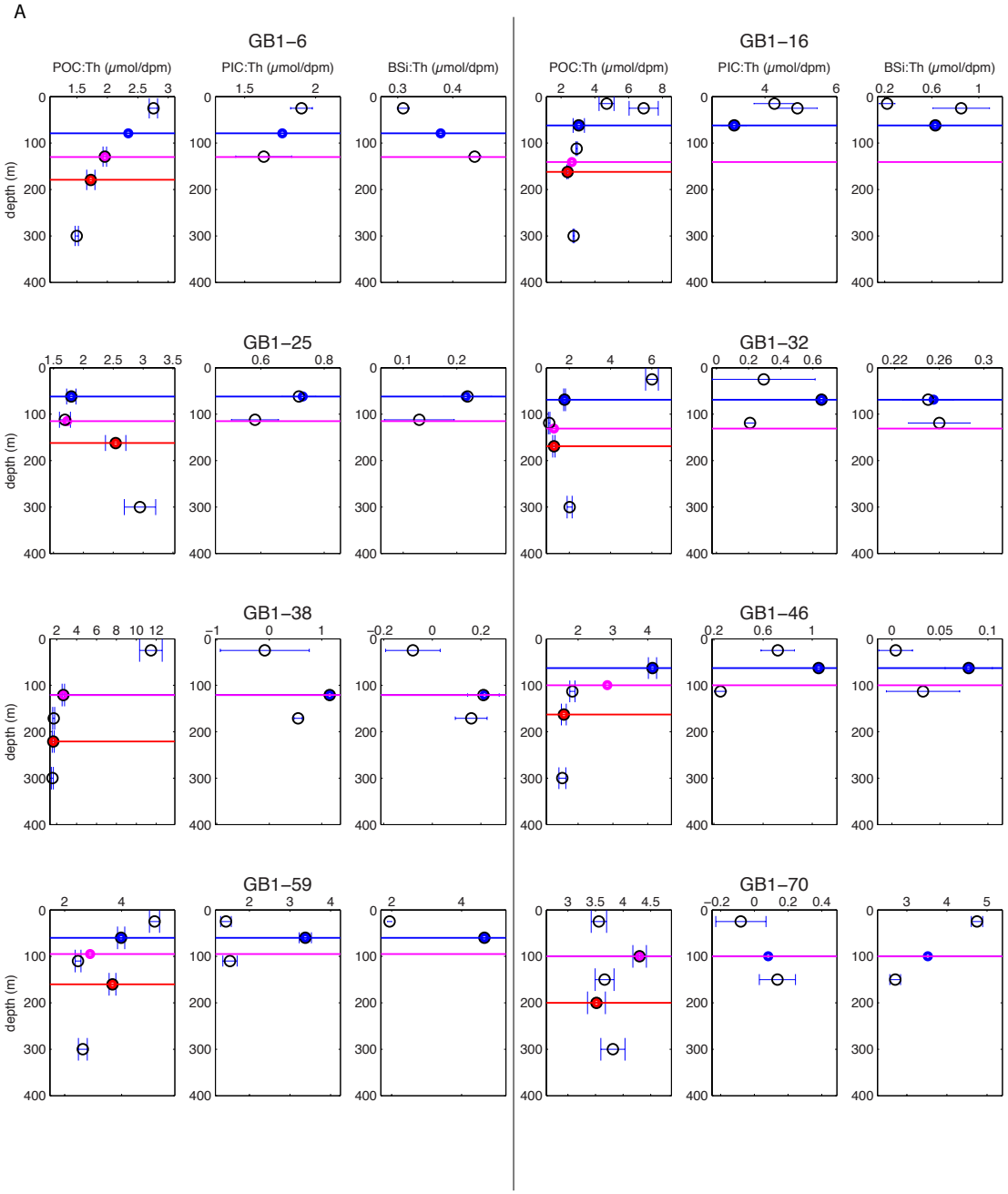
A
GB1–6
POC:Th (μmol/dpm)
PIC:Th (μmol/dpm)
BSi:Th (μmol/dpm)
GB1–16
GB1–25
GB1–32
GB1–38
GB1–46
GB1–59
GB1–70
depth (m)

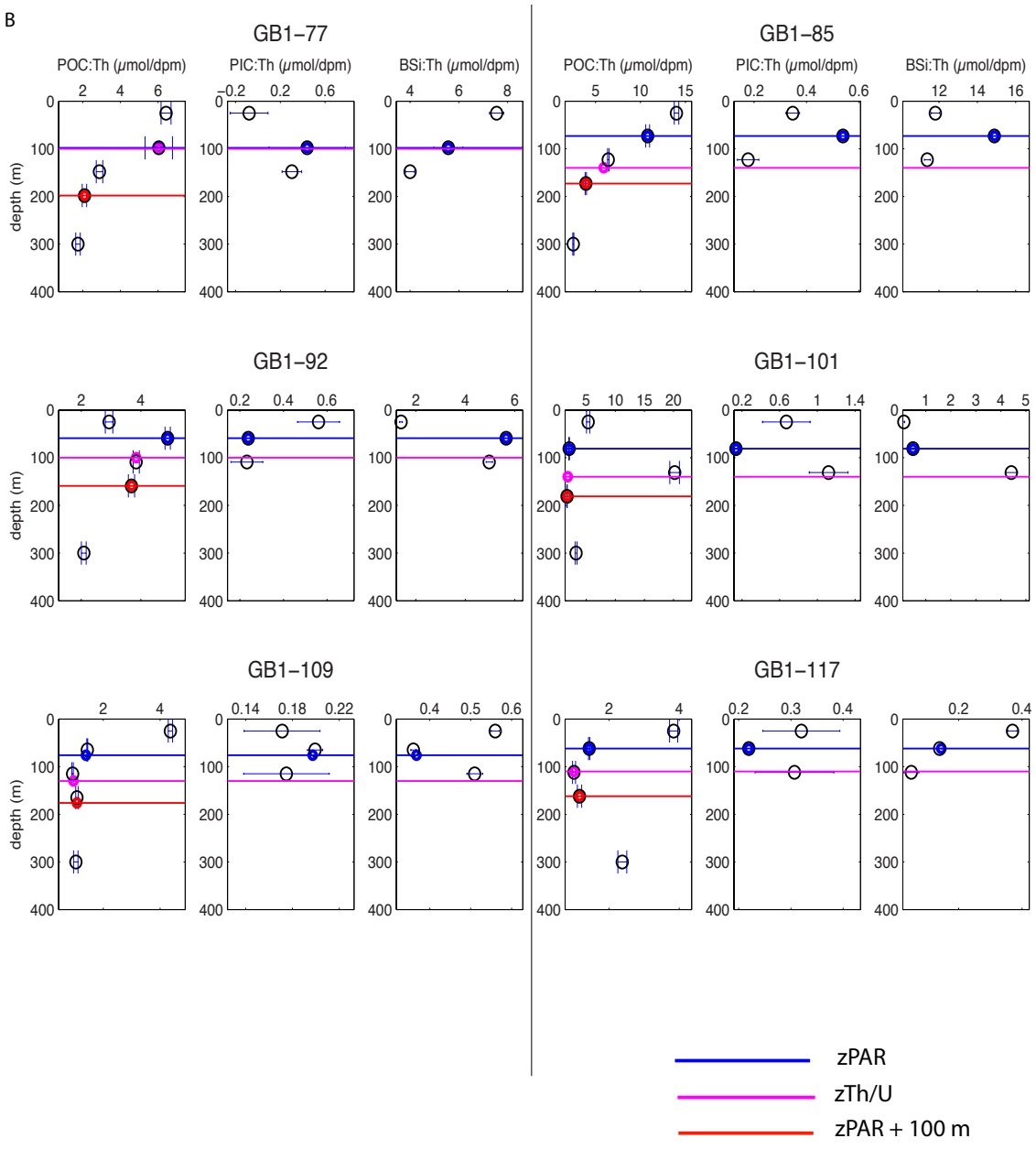
B
GB1–77
GB1–85
GB1–92
GB1–101
GB1–109
GB1–117
POC:Th (μmol/dpm)
PIC:Th (μmol/dpm)
BSi:Th (μmol/dpm)
depth (m)
zPAR
zTh/U
zPAR + 100 m

C

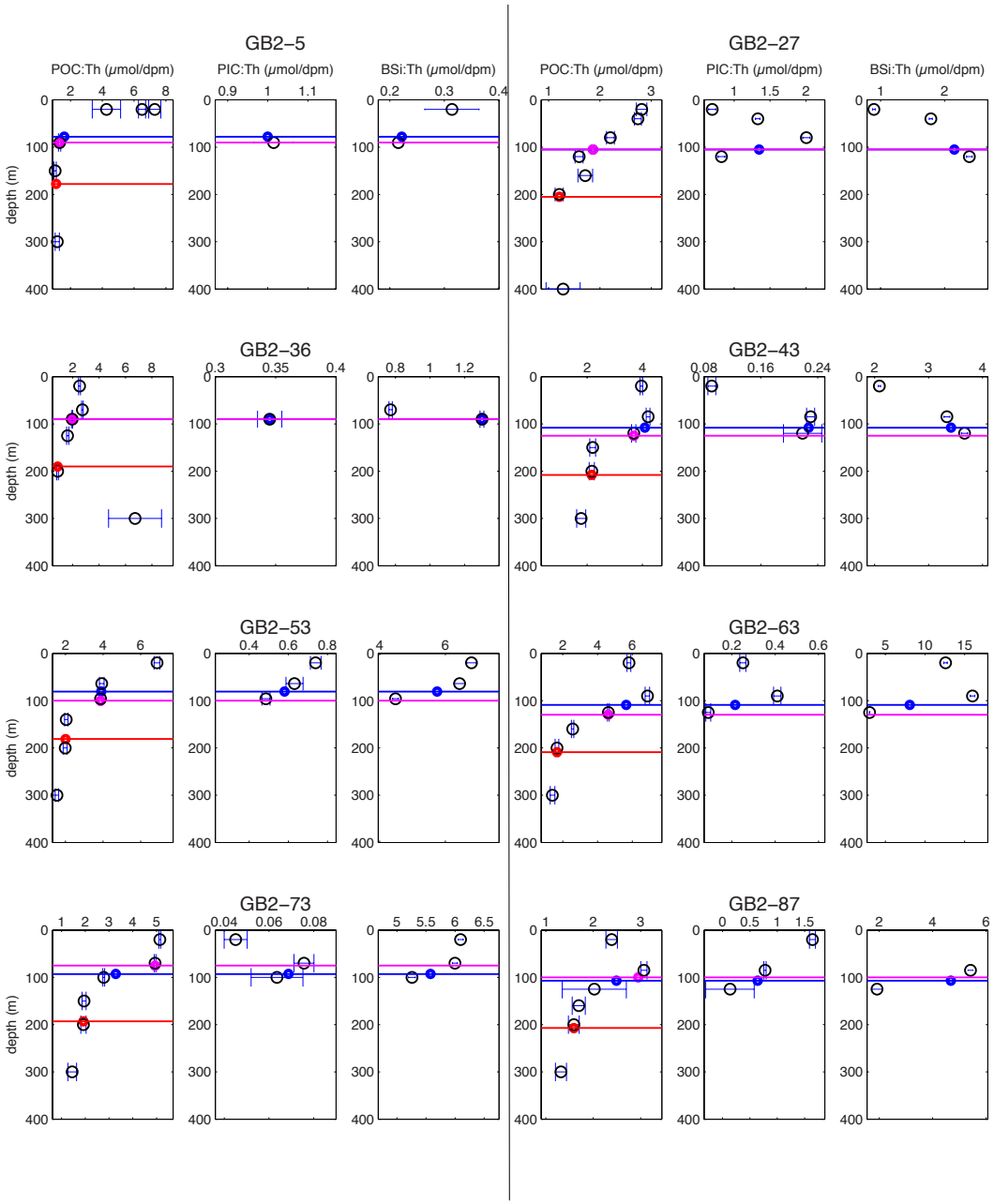
GB2–5
GB2–27
GB2–36
GB2–43
GB2–53
GB2–63
GB2–73
GB2–87
POC:Th (μmol/dpm)
PIC:Th (μmol/dpm)
BSi:Th (μmol/dpm)
depth (m)

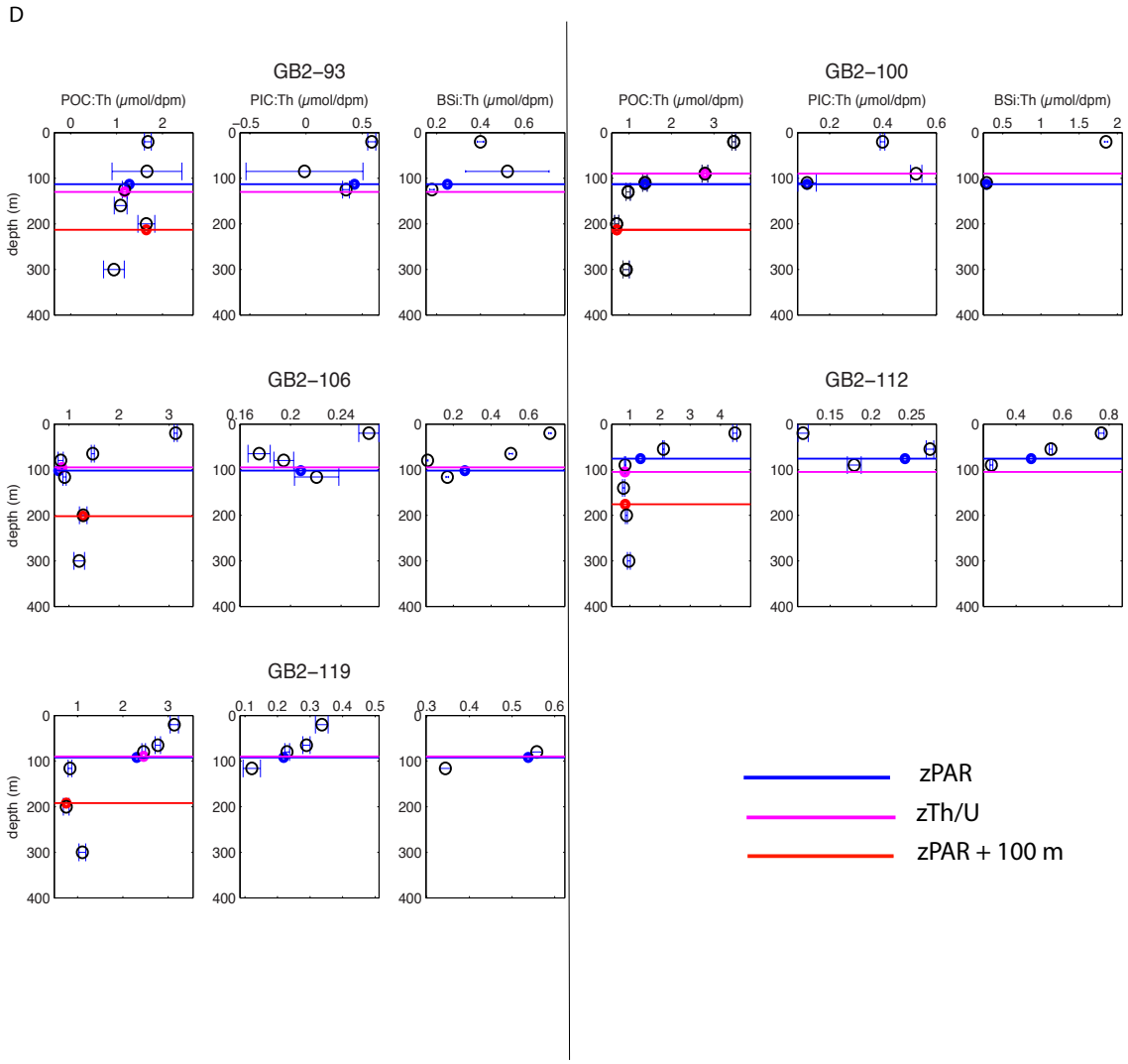

Figure S1. Profiles of >51 μm POC:^{234}Th, PIC:^{234}Th and BSi:^{234}Th above 400 m. Black open circles represent measurements. Colored circles represent values at three possible depths (colored lines; see legend) in the POC:^{234}Th panels, and at z_{PAR} (blue line) for the PIC:^{234}Th and BSi:^{234}Th panels. These values were interpolated when there were no measurements at these depths (refer to Tables 2 and 3 for specific stations). At station GB2-106, the BSi:^{234}Th interpolation calculation excluded the anomalously low value at 80 m. Error bars shown are the propagated errors of >51 μm [POC], [PIC], [BSi] and particulate ^{234}Th activity measurements. Note that "negative" values are below the instrument detection limit (see Sect. 2.3), and are equal to 0 within error.

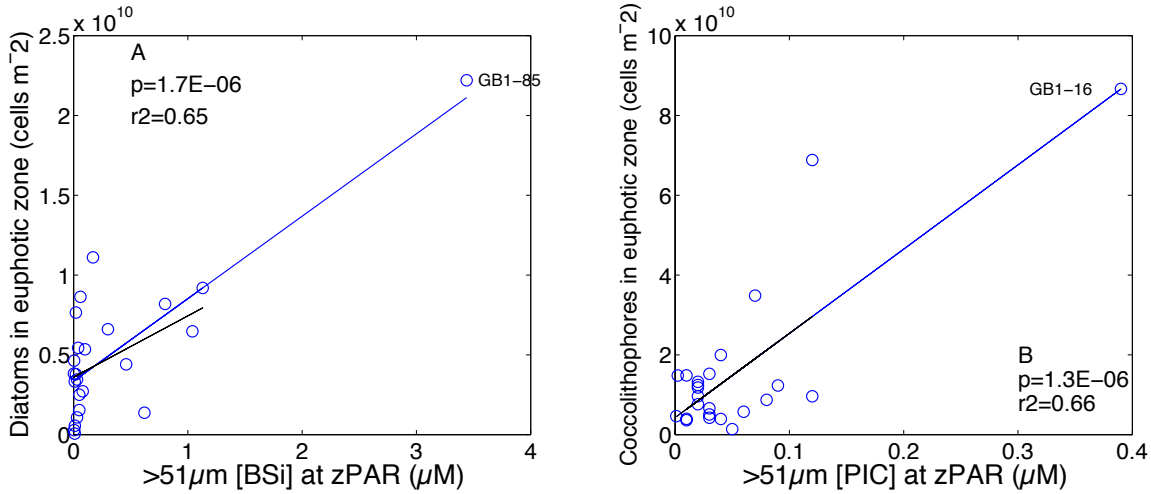

Figure S2. (A) Diatom cell counts integrated from surface to z_{PAR} (cells m^{-2}) as a function of >51 µm [BSi] at z_{PAR}. (B) Integrated coccolithophore cell counts as a function of >51 µm [PIC] at z_{PAR}. Outliers for >51 µm [BSi] and [PIC] at stations GB1-85 and GB1-16, respectively, are defined according to Chauvenet's Theorem (Glover et al., 2011). Total euphotic zone cell counts of diatoms and coccolithphores are significantly correlated to >51 µm [BSi] and [PIC] at z_{PAR} , respectively. The significant linear relationships are plotted here as blue lines, with corresponding p and r^2 values indicated. The regressions remain significant ($p<0.05$) even when excluding the outliers GB1-85 (Fig. S2a) and GB1-16 (Fig. S2b) from analysis (black lines). We note that cell counts are only available for the <36 µm size-fraction because of the methodology used for enumeration (see Supplemental Methods), while the biomineral measurements are of the >51 µm particle size-fraction (Sect. 2.2). Nonetheless, these relationships suggest that the >51 µm [BSi] and [PIC] at z_{PAR} do scale with the abundance of diatoms and coccolithophores in the euphotic zone of the water column.

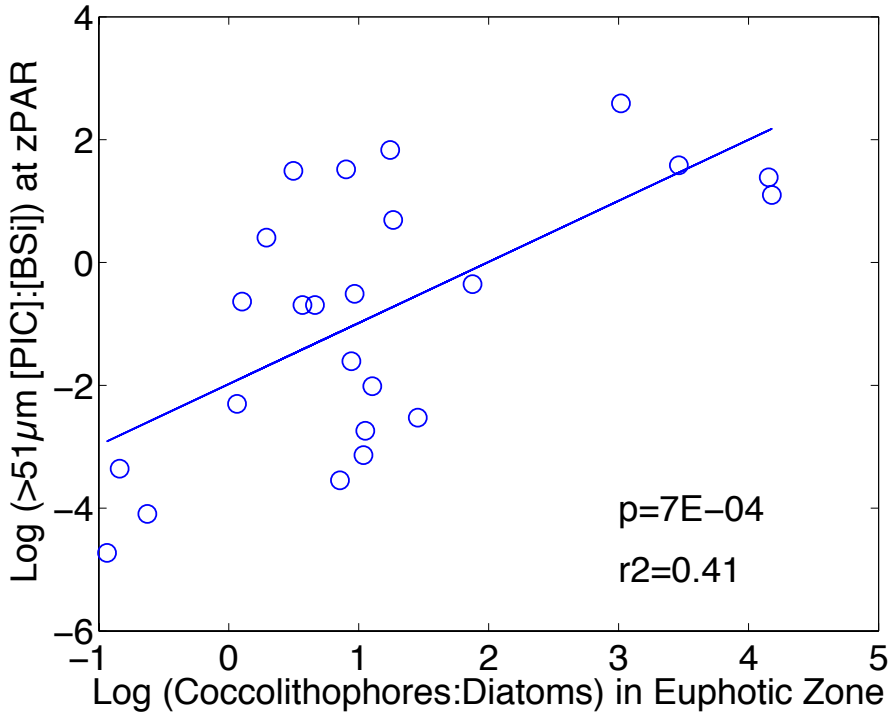

Figure S3. The natural log of the ratio of >51 μm [PIC]:[BSi] at z_{PAR} as a function of the natural log of the ratio of integrated coccolithophore: diatom cell counts in the euphotic zone. The significant linear relationship is plotted as a blue line, with a corresponding p and r^2 value indicated. This further supports the application of >51 μm size-fraction biomineral concentrations at z_{PAR} as a proxy for describing euphotic zone ecosystem composition in Sect. 4.7 and Fig. 10. Despite the different size-fractions that are represented by the biomineral measurements and the cell counts (see Supplemental Methods), the significant correlation nonetheless supports the use of >51 μm biomineral concentration ratios to describe the proportional abundance of certain phytoplankton types.

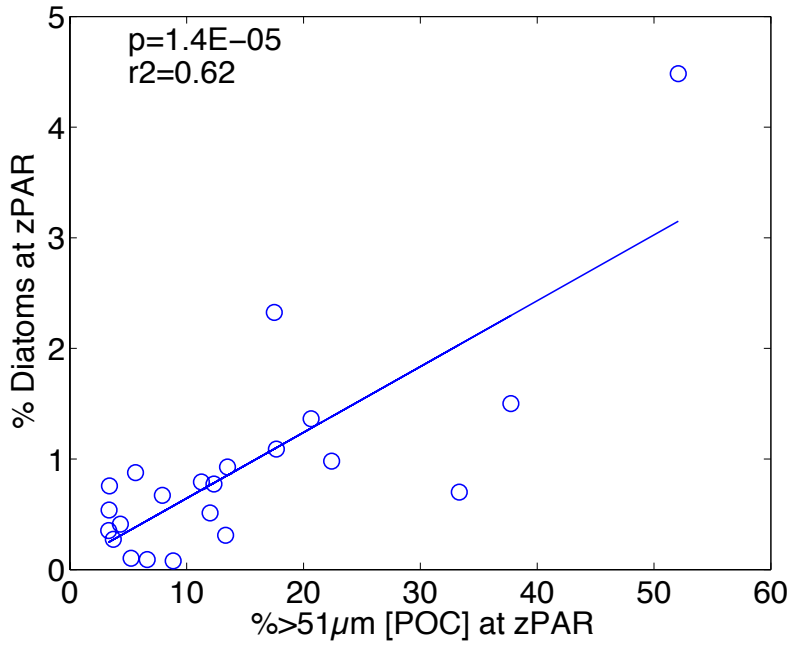

Figure S4. Percentage of total cells that are diatoms at z_{PAR} as a function of the % >51 µm [POC] at z_{PAR}. The significant linear relationship is plotted as a blue line, with a corresponding p and r^2 value indicated. This relationship shows that FlowCAM® measurements of diatom abundance support our interpretation that the size fractionation of POC (% >51 µm [POC] at z_{PAR}) determined from in-situ pump particle measurements (Sect. 2.2) reflects the relative abundance of diatoms. We note that there is no significant relationship between relative coccolithophore abundance and the size fractionation of POC.

Supplementary Methods for Figs. S2-S4

The FlowCAM® imaging cytometer enumerated nano- and microplankton cells from 10 mL Niskin cast samples at all McLane pump stations except GB2-36, GB2-27 and GB2-119 (refer to Table 1 for station locations) (Poulton and Martin, 2010). Moreover, at stations GB1-38 and GB1-70, cell counts were missing at z_{PAR}, and only measured at depths above and below z_{PAR}. The size range of counts was 5.6-35.5 μm. While particles >36 μm (up to 200 μm) could be seen in the FlowCAM®, they were rare in 10 mL samples, such that their normalized abundance could not be accurately calculated. Total diatom cell counts in the euphotic zone were approximated by summing FlowCam® -derived diatom concentrations (cells/mL) at all depths above z_{PAR}:

$$\text{total cell counts} = \sum_{1}^{\text{end}} \text{mean}\left[\frac{\text{cells}}{\text{mL}}_{n}, \frac{\text{cells}}{\text{mL}}_{n-1}\right] \times [z_n - z_{n-1}]$$

where n is the measurement index number from the surface depth at n=1 downward towards z_{PAR} at n="end". The unit for this summation is equivalent to cells m^{-2}. Coccoliths and plated cells in the same Niskin samples were counted by birefringence microscopy (Balch et al., 2011). Total coccolithophore counts in the euphotic zone (cells m^{-2}) were similarly estimated by summing the microscopy-based concentrations at all depths above z_{PAR}.

Supplementary References

Balch, W. M., Drapeau, D. T., Bowler, B. C., Lyczskowski, E., Booth, E. S., and Alley, D.: The contribution of coccolithophores to the optical and inorganic carbon budgets during the Southern Ocean Gas Exchange Experiment: New evidence in support of the Great Calcite Belt hypothesis, J. Geophys. Res., 116, C00F06, 2011.

Glover, D. M., Jenkins, W. J., and Doney, S. C.: Modeling methods for marine science., Cambridge University Press, 2011.

Poulton, N. J., and Martin, J. L. Imaging flow cytometry for quantitative phytoplankton analysis - FlowCAM. In: Karlson B, Cusack C, Bresnan E (eds) Microscopic and molecular methods for quantitative phytoplankton analysis, Vol Chapter 8. Intergovernmental Oceanographic Commission of UNESCO, Paris, France, 49-54, 2010.